
# Faintest of the brightest- GRB Hunters

**Sarvesh Kulkarni**

Mentor: Gaurav Waratkar and
Meghna Dixit

Krittika Summer Projects(KSP)
Krittika astronomy community

Indian Institute of Technology Bombay

**June, 2023**

# Contents


**1 Introduction** **1**

**2 Problem Statement** **3**

**3 Computation** **5**

**4 Goal** **7**

**5 Literature** **8**

**6 Algorithm** **9**

**7 GRB210709A** **11**
- 7.1 Raw Light Curves . . . 11
- 7.2 Outliers . . . 11
- 7.3 SNRs of GRB region . . . 13
- 7.4 SNRs of non-GRB region . . . 13
- 7.5 Confidence Number . . . 14
- 7.6 Conclusion . . . 14

**8 GRB210519A** **15**
- 8.1 Raw Light Curves . . . 15
- 8.2 Outliers . . . 15
- 8.3 SNRs of GRB region . . . 17
- 8.4 SNRs of non-GRB region . . . 17
- 8.5 Confidence Number . . . 18
- 8.6 Conclusion . . . 18

# List of Figures


1.1 Gamma-ray-burst Mechanism . . . . . 1

3.1 GRB190928A . . . . . 5

7.1 GRB210709A raw light curve at time bin 0.1s . . . . . 11
7.2 20-200keV . . . . . 12
7.3 100-200keV . . . . . 12
7.4 50-100keV . . . . . 12
7.5 SNR vs time bin for grb window . . . . . 13
7.6 SNR vs time bin for non-grb window . . . . . 13

8.1 GRB210519A raw light curve at time bin 0.1s . . . . . 15
8.2 20-200keV . . . . . 16
8.3 100-200keV . . . . . 16
8.4 50-100keV . . . . . 16
8.5 SNR vs time bin for grb window . . . . . 17
8.6 SNR vs time bin for non-grb window . . . . . 17

# List of Abbreviations

**GRB** Gamma-Ray Burst . . . . . 1
**CZTI** Cadmium Zinc Telluride Imager . . . . . 3
**SNR** Signal-to-Noise Ratio . . . . . 3
**lc** Lightcurve . . . . . 5

# 1

# Introduction

Gamma-Ray Bursts (hereafter GRBs) are short and intense pulses of soft $\gamma$-rays. The bursts last from a fraction of a second to several hundred seconds, marking the birth of a black hole. The overall observed fluences range from Gamma-Ray Burst (GRB) are $10^{-4}$ $erg/cm^2$ to $10^{-7}$ $erg/cm^2$ which corresponds to isotropic luminosity of $10^{51} - 10^{52}$ $erg/s$, making GRBs the most luminous objects in the sky.

Emission from GRBs is divided in two phases. Prompt Emission is the initial phase of bright and highly variable radiation in the kiloelectron volt-to-megaelectronvolt band where it releases most of its energy, which is probably produced within the jet and lasts from milliseconds to minutes. Followed by Afterglow emission caused by the interaction of the jet with the surrounding medium generates shock waves which lasts from days to months and occurs over a broad energy range from the radio to the gigaelectronvolt bands . Afterglow emission is generally well explained as synchrotron radiation emitted by electrons accelerated by the external shock. GRBs are classified into two types -

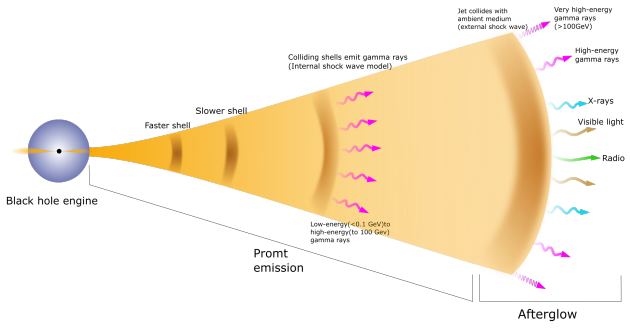


Figure 1.1: Gamma-ray-burst Mechanism

Long GRBs and Short GRBs. When the duration of prompt emission is more than 2s and are result of the death of a massive star, that has a very short lifetime of 10 million years. The implosion of such stars owing to their enormous gravity forms a black hole in its core and releases Long GRBs that are expected to originate in stellar nurseries which are located in spiral arms of spiral galaxies.

And when the duration of prompt emission is less than 2s are formed during the merger of binary neutron stars forming black holes, in an extremely short duration and produce Short GRBs. A system

of binary stars takes billions of years to form. Therefore, Binary neutron stars are expected to be found in dead elliptical galaxies.

# 2

# Problem Statement

The issue at hand is the requirement for a dependable and accurate quantification of GRB detections made by the Astrosat's Cadmium Zinc Telluride Imager (CZTI). GRBs are high-energy gamma-ray bursts that originate from distant celestial sources and provide crucial insights into high-energy astrophysics. Astrosat, India's first multi-wavelength satellite observatory, was instrumental in detecting and studying these astrophysical phenomena. However, establishing a robust quantification methodology for Cadmium Zinc Telluride Imager (CZTI)'s GRB detections is a crucial need in order to improve the precision and reliability of the collected data.

The current challenge is measuring the properties and characteristics of GRBs captured by CZTI accurately. Despite the fact that CZTI is a sophisticated instrument capable of recording high-energy events, quantification of GRB detections remains a difficult task due to a number of factors. These factors include the inherent variability of GRBs in terms of duration, intensity, and spectral properties. Furthermore, CZTI sensitivity and background noise levels must be carefully considered in order to distinguish genuine GRB signals from spurious noise or instrumental anomalies. Failure to develop an accurate quantification methodology can result in incorrect interpretations.

In addition to addressing the challenges mentioned above, our research will involve comprehensive testing of various methods for calculating the Signal-to-Noise Ratio (SNR) of GRB detections in Astrosat's CZTI data. Including, modeling the noise as Gaussian and considering the total counts of signal and noise among other methods. Additionally, we recognize the impact of bin size on SNR values and its potential to influence the reliability of the measurements. The results of these investigations will provide valuable insights into the quantification of Signal-to-Noise Ratio (SNR) in CZTI's GRB detections. By comparing different methodologies and studying the influence of bin size, we will be able to assess the strengths and limitations of each approach, ultimately justifying the chosen methodologies for accurate SNR estimation.

The development of a reliable quantification methodology for GRB detections in Astrosat's CZTI data will have significant implications. We can effectively distinguish weaker events from noise or spurious signals by accurately quantifying GRBs. This capability is crucial for distinguishing genuine GRBs from false positives. The validated quantification methodology will not only help us better understand GRB properties, but it will also be a useful tool for future CZTI GRB detections. It will help to refine data analysis techniques and aid in the identification and characterization of a

broader range of GRBs, advancing our understanding of these astrophysical phenomena.

To summarize, the primary problem statement is to identify whether the given detection is infact a GRB or a particle event. Then attach a confidence number to it.

# 3

# Computation

For the computation aspect of this project, Ubuntu-20.04.6 was used to perform the necessary data processing tasks. The first step involved installing the pipeline required for the analysis of Astrosat's CZTI data. The version V2.1 was implemented as the newer V3.0 was not tested properly. The procedure in the user manual was followed to the point.

Once the pipeline was successfully installed, we proceeded to run the relevant modules to create lightcurve(lc) files for GRB190928A (one of the brightest GRB detected). Plotting the Lightcurve (lc) files to visualise the GRB events was one of the first steps in the analysis. The plot of 'rate' vs 'time' displayed the bright GRB.

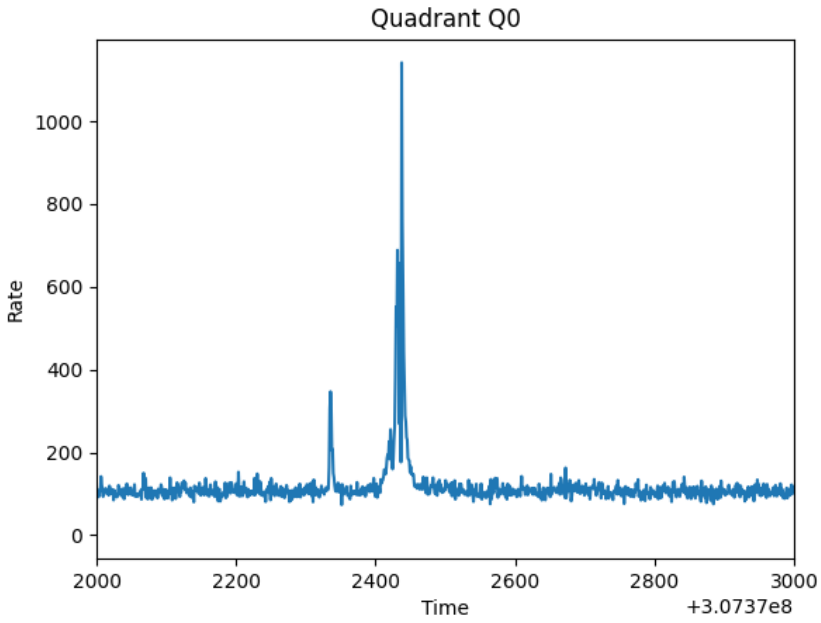


Figure 3.1: GRB190928A

Following the lc plot analysis, we focused on the SNR calculation, an essential aspect of GRB quantification. We applied the appropriate techniques, considering factors such as background noise levels and signal counts, to determine the SNR values for the detected GRBs.

The SNR analysis aimed to assess the significance of the GRB signals relative to the background noise. By quantifying the SNR, we gained a measure of the reliability and strength of the GRB detections. This step was crucial in distinguishing genuine GRBs from noise or instrumental artifacts, thereby ensuring the accuracy and validity of the quantification process.

# 4

# Goal

Our primary goal is to enhance the confidence and accuracy of GRB detections in Astrosat's CZTI data. To achieve this, we have outlined a specific plan of action. Firstly, we will compare and evaluate different SNR calculation methods. By systematically assessing and comparing these methods, we aim to identify the most reliable and effective approach for quantifying the GRB detections. This analysis will enable us to increase our confidence in the validity of the identified GRB signals.

Additionally, we intend to explore the impact of changing the bin size on the SNR values. By systematically varying the bin size and observing the corresponding changes in SNR, we can gain insights into how different binning schemes influence the reliability and accuracy of GRB quantification. Through this investigation, we seek to understand the underlying reasons behind any observed variations in the SNR values.

By accomplishing these goals, we aim to improve the overall quantification of GRB detections in Astrosat's CZTI data. This will provide a more robust foundation for identifying genuine GRBs and distinguishing them from false positives or noise. Ultimately, the research will contribute to advancing the reliability and accuracy of GRB studies using the CZTI instrument, enabling deeper insights into the nature of these astrophysical phenomena.

# 5

# Literature

We thoroughly explored relevant literature by following key links in our attempt for a thorough understanding of the field. The first link we followed led us to the comprehensive Wikipedia page on GRBs This authoritative source provided a basic overview of GRBs, including their properties, classification, and scientific research in this field.

Continuing our exploration, we accessed a research article titled "The Cadmium Zinc Telluride Imager on AstroSat". This scholarly paper presented insights into the engineering and mechanical aspects of CZTI as an instrument. It gives a detailed overview of how the different quadrants of CZTI work and how the detector converts the incident photons into electrical signals for detection. It offered valuable information on CZTI's capabilities, data analysis techniques, and the challenges encountered by CZTI.

Additionally, we examined a research paper available on arXiv, titled "The Search for Fast Transients with CZTI." This paper introduced us to the various modules in the pipeline, required to clean and optimize the raw data.

By following these links, we accessed a range of literature sources, including authoritative references, research articles, and observational studies, to broaden our knowledge and understanding of GRB detection and quantification. This literature review process ensured a comprehensive foundation for our research and informed our subsequent methodology development and analysis of Astrosat CZTI GRB detections.

# 6

# Algorithm

1. **Opening and Filtering Data–** We access the raw data stored in lc files in this first stage. The Savitzky-Golay (savgol) filter is used to detrend the data in order to increase the signal-to-noise ratio and enable further analysis.

2. **Outlier Detection with IQR–** Following the filtering of the data, the next step is to identify possible GRB occurrences using outlier detection. Outliers are data points that differ greatly from the normal distribution of data. The Interquartile Range (IQR) approach was used in this algorithm because it is resilient against extreme values and well-suited for spotting outliers in many forms of data, including light curves. For the combined energy window of 20-200 KeV, an outlier is defined as any data point that lies beyond a threshold of 4 times the IQR. Similarly, for the narrower energy ranges of 100-200 KeV and 20-100 KeV, the threshold is set at 3 times the IQR. By setting different thresholds for each energy range, we account for variations in the data's statistical properties and ensure accurate outlier detection.

3. **Plotting Outliers–** After identifying the potential GRB events as outliers in the filtered light curves, the scatter plots are created to visually represent their occurrence. In accordance with the four Quadrants of the CZTI instrument, four plots for each energy range are plotted. Additionally, separate scatter plots for each of the three energy ranges are plotted: 20-200 keV, 100-200 keV, and 20-100 keV. In this case, the lower energy range of 20-50 keV are not taken into account for calculating the outlier, since this range is the most susceptible to noise. These scatter plots provide a comprehensive view of the detected outliers, helping us analyze their characteristics and potential relationships with other features in the data. The distinct energy range plots allow us to study how GRB events manifest at different energy levels and unveil possible energy-dependent phenomena.

4. **Identifying GRBs–** To identify a genuine GRB, we apply a strict criterion that requires the event to be an outlier in at least two of the twelve scatter plots created in the preceding phase. This criterion assures that only important occurrences are consistently classified as outliers in a variety of situations, reducing false positives. The validity of the GRB identification is increased by requiring events to behave exceptionally in several energy ranges and quadrants. This phase is essential for removing noise-induced false detections and improving the algorithm's precision.

5. **Calculating SNR Values–** The SNRs for the probable GRB event are then determined in a variety of time bins once the potential GRB events have been detected. The SNR values are essential for understanding the importance of the discovered events and their temporal properties in the context of GRBs.

   The formula used for calculating the SNR is

   $$SNR = (((signalstrength - backgroundstrength) * scale)/sigma) \tag{6.1}$$

   Where the signal strength is the peak value in the GRB window and the background strength is taken as the mean value of background count of the pre-burst and post-burst region of the GRB. The sigma is the mean of the two standard deviation of these pre-burst and post-burst background count. SNR values are computed for particular time bins, such as 0.2, 0.4, 0.6, 0.8, 1, 5, and 10 seconds. We can examine the temporal development of GRBs and how their signal intensities change across various time scales thanks to these time bins. We can more accurately define the length and intensity of GRB occurrences by calculating the SNR in each time bin.

6. **Plotting SNR Values by Quadrants–** To gain a deeper understanding of the temporal distribution of SNRs, they are grouped by the quadrants and then plotted with respect to the time bin sizes.

   This analysis may reveal intriguing patterns, such as the ideal time bin for the GRB. By plotting SNR values in this manner, we can gain valuable insights into the temporal aspects of GRBs and their potential astrophysical implications.

7. **Non-GRB Window and SNR Calculation–** To accurately classify the given event as GRB or particle event and compare its significance corresponding to the noise, the previous step 5 is followed for a region with no significant event. The SNR values are calculated for a non-'GRB' window. These SNR values are then use to compare with the SNR values of the 'GRB' window.

8. **Calculating the Confidence Number–** The final step involves calculating the confidence number, which provides a quantitative measure of the confidence level for the detected GRB event. To do this, the mean value of the SNR for the identified 'GRB' window and the mean value of the SNR for the non-'GRB' window.

   The credibility of the GRB detection is increased by a greater confidence number percentage, which denotes a stronger signal in comparison to background noise.

   $$\begin{aligned} ratio &= SNRnonGRB/SNRGRB \\ value &= 1 - ratio \\ percentage &= value * 100 \end{aligned} \tag{6.2}$$

   Where the SNRnonGRB is the mean value of SNR for the non-GRB window and SNRGRB is for the GRB window.

....

# 7

# GRB210709A

## 7.1 | Raw Light Curves

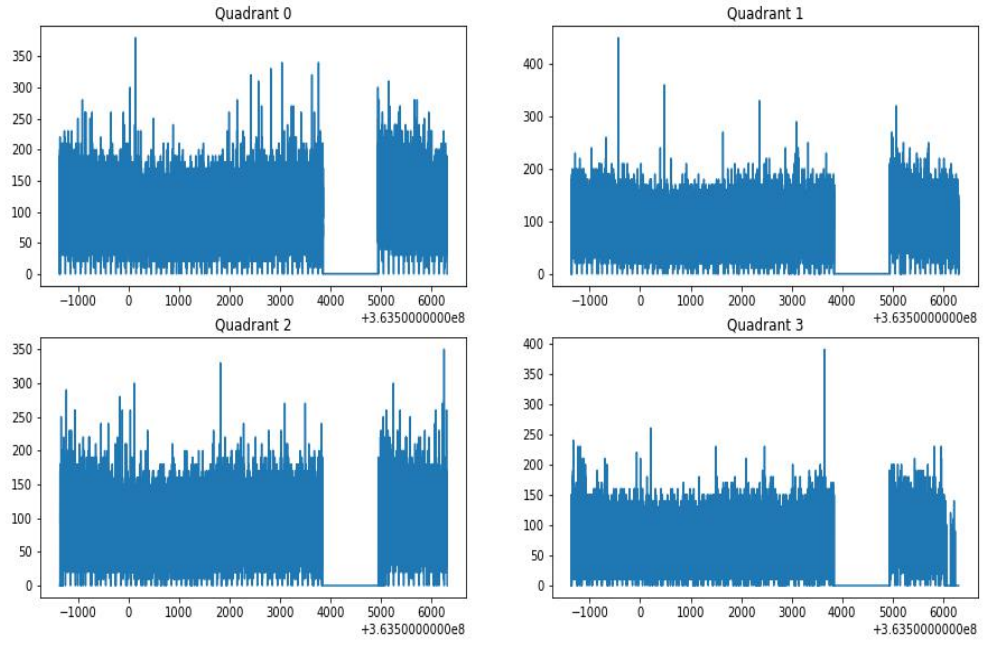


Figure 7.1: GRB210709A raw light curve at time bin 0.1s

The next step is to filter the data and get the outliers using the Interquartile range(IQR). The plots are shown in the next figure. In the given range, the outlier was found in two plots and hence was classified as a GRB. The plots are catergorized in three energy range.

## 7.2 | Outliers

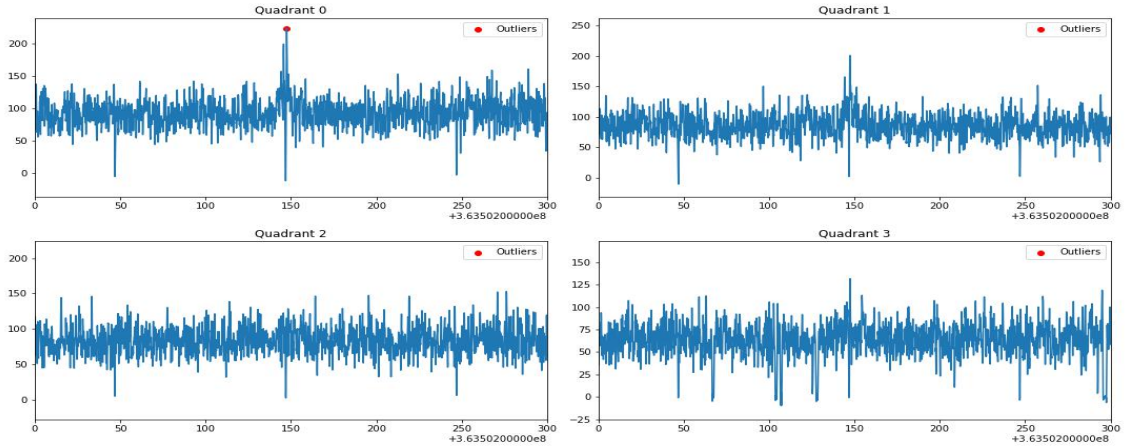


Figure 7.2: 20-200keV

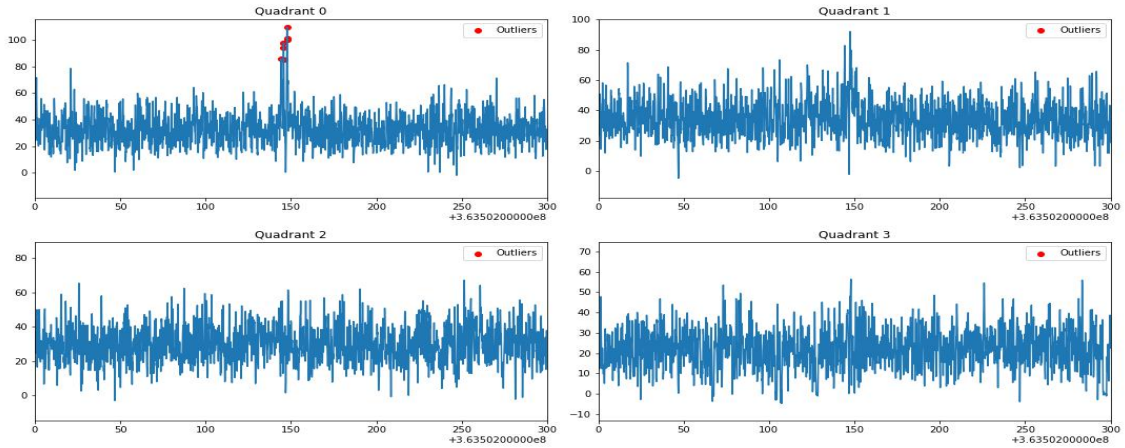


Figure 7.3: 100-200keV

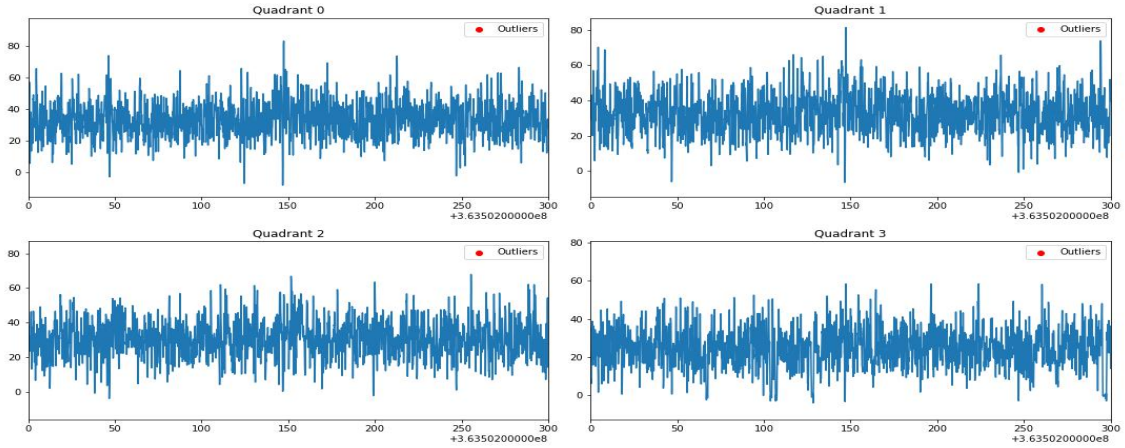


Figure 7.4: 50-100keV

## 7.3 | SNRs of GRB region

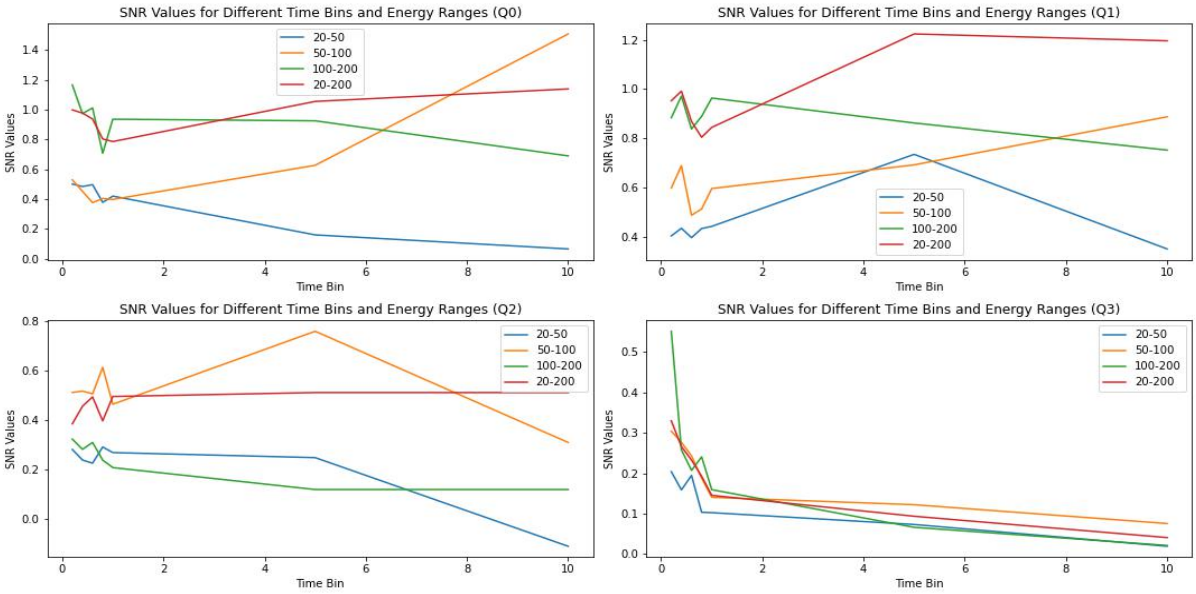


Figure 7.5: SNR vs time bin for grb window

Here the graphs of the SNR values of the suspected GRB window across various time bins are plotted. They are grouped by the energy ranges. The Quadrant 0, Quadrant 1 and Quadrant2 of the SNRs of the GRB region show a solid trend while the Quadrant 3 fails to capture the suspected GRB.

## 7.4 | SNRs of non-GRB region

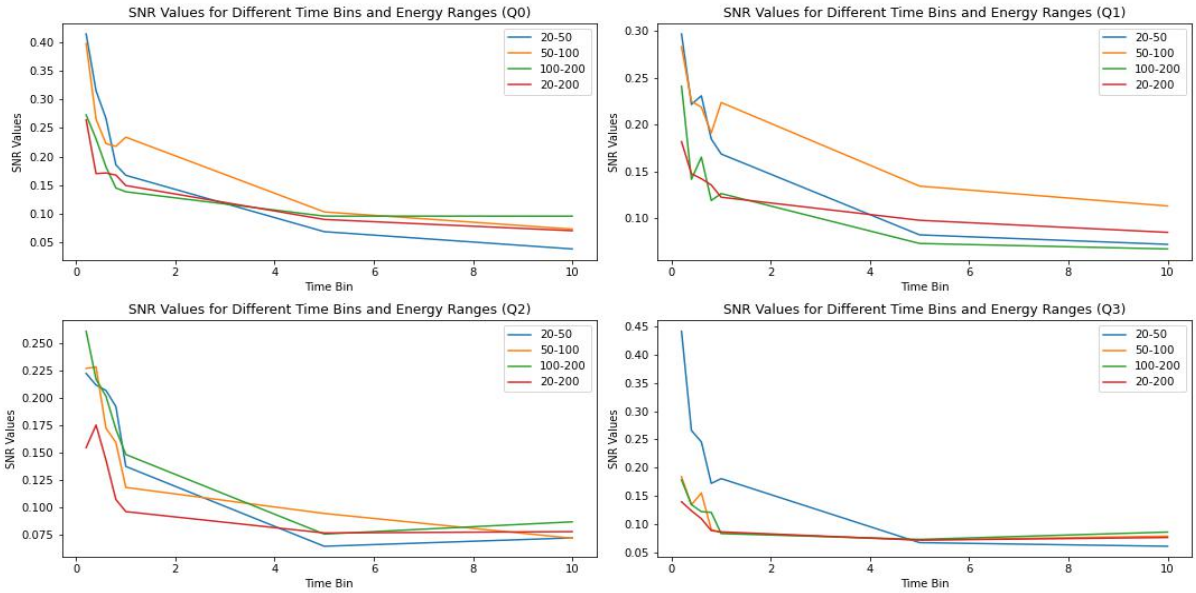


Figure 7.6: SNR vs time bin for non-grb window

The graphs of the SNR of a window which has no significant event in that particular window are plotted across various time bins. They are again grouped by the energy ranges. All the quadrants show a similar profile of SNR which is distinct from the graphs of the GRB window.

## 7.5 | Confidence Number

The ratio of the SNRnonGRB and SNRGRB value is around 0.32. Hence, a confidence value that can be associated to this detection of the GRB through this algorithm is 68.26%.

## 7.6 | Conclusion

The given detection is identified as GRB by this algorithm and a confidence value of 68.26% can be associated to it.

# 8

# GRB210519A

## 8.1 | Raw Light Curves

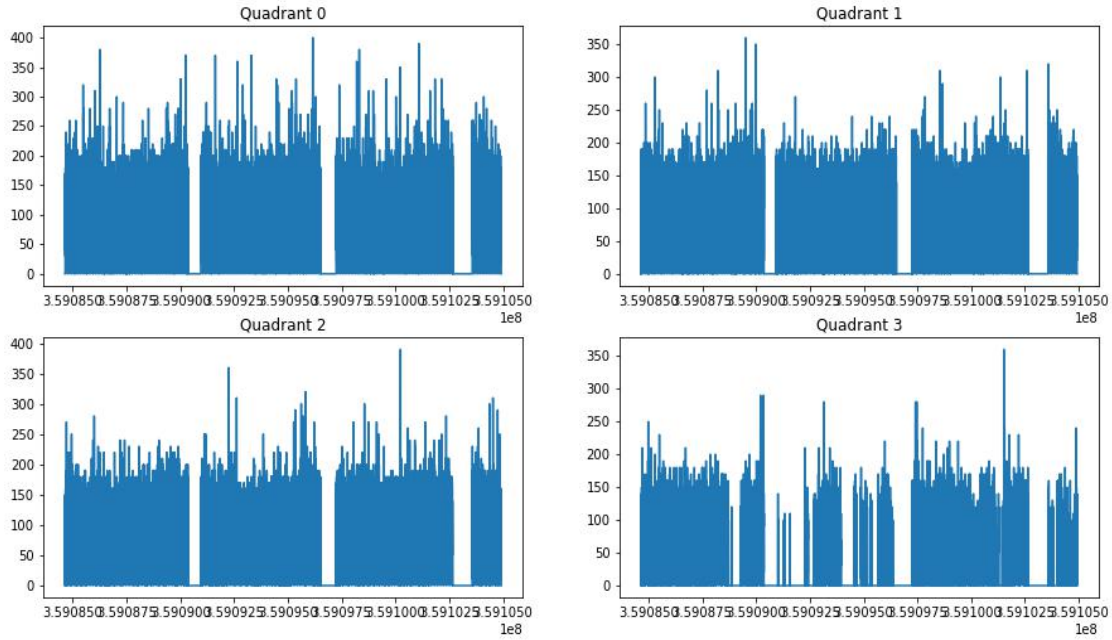


Figure 8.1: GRB210519A raw light curve at time bin 0.1s

The next step is to filter the data and get the outliers using the Interquartile range(IQR). The plots are shown in the next figure. In the given range, the outlier was found in one single plot and hence was classified as a particle event. The plots are catergorized in three energy range.

## 8.2 | Outliers

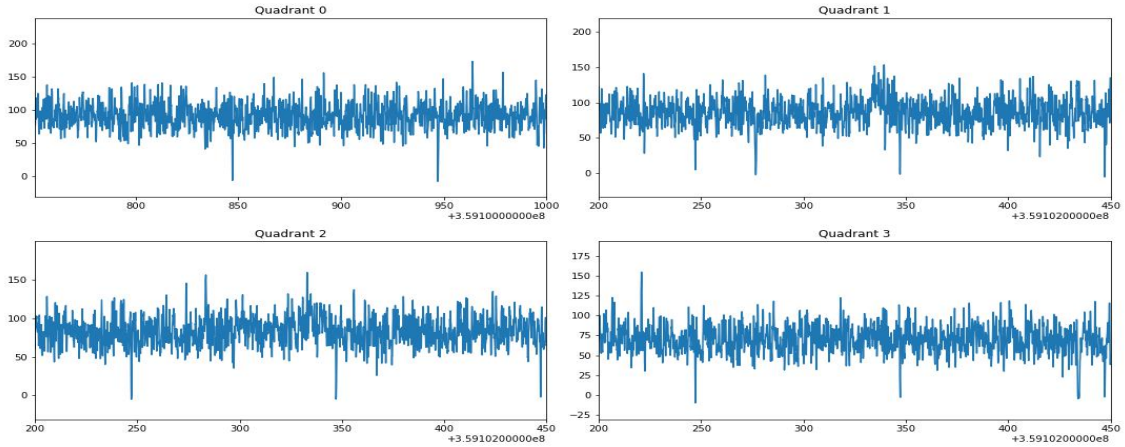


Figure 8.2: 20-200keV

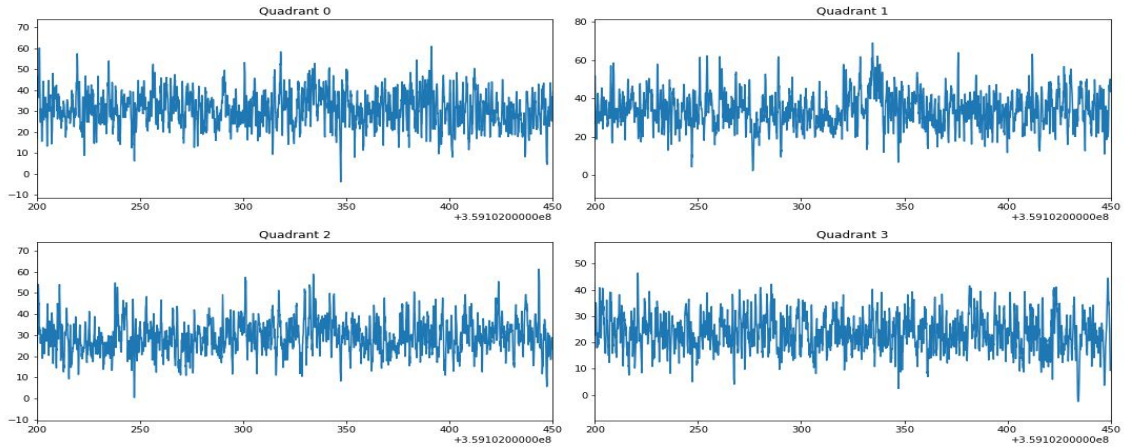


Figure 8.3: 100-200keV

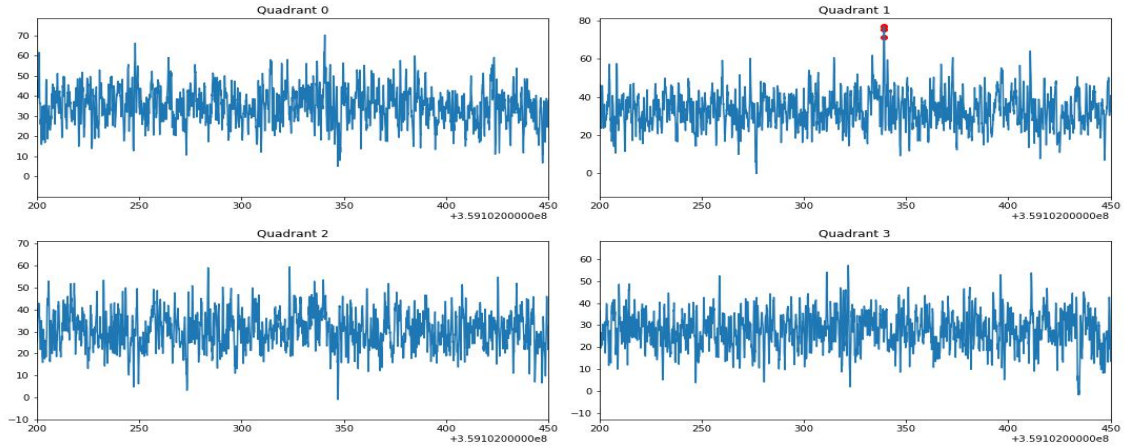


Figure 8.4: 50-100keV

## 8.3 | SNRs of GRB region

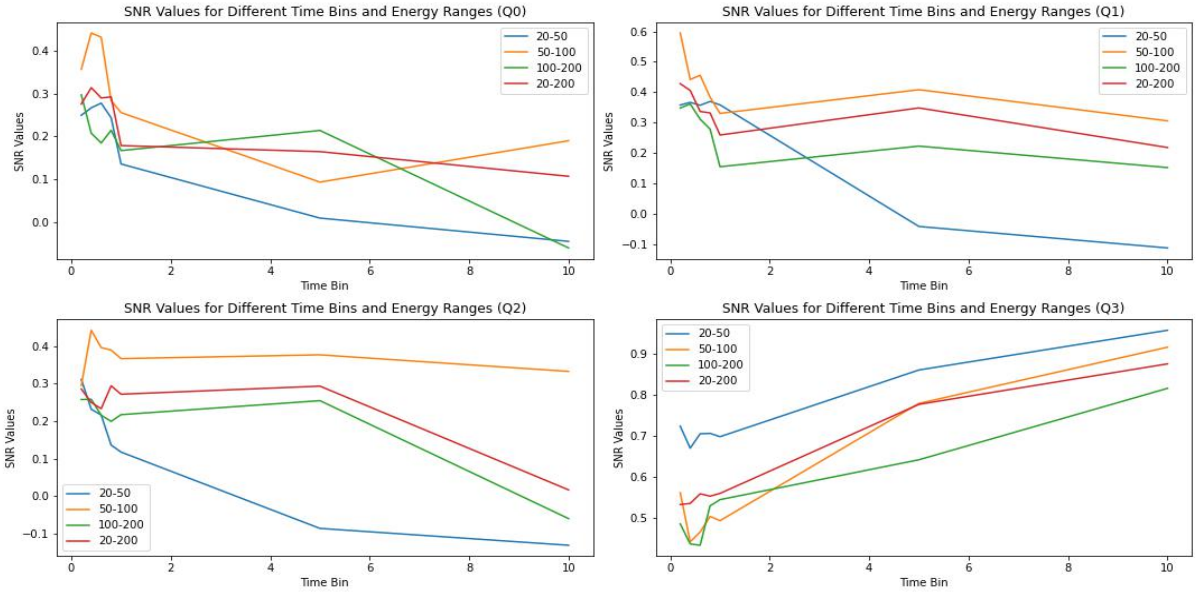


Figure 8.5: SNR vs time bin for grb window

Here the graphs of the SNR values of the suspected GRB window across various time bins are plotted. They are grouped by the energy ranges.

## 8.4 | SNRs of non-GRB region

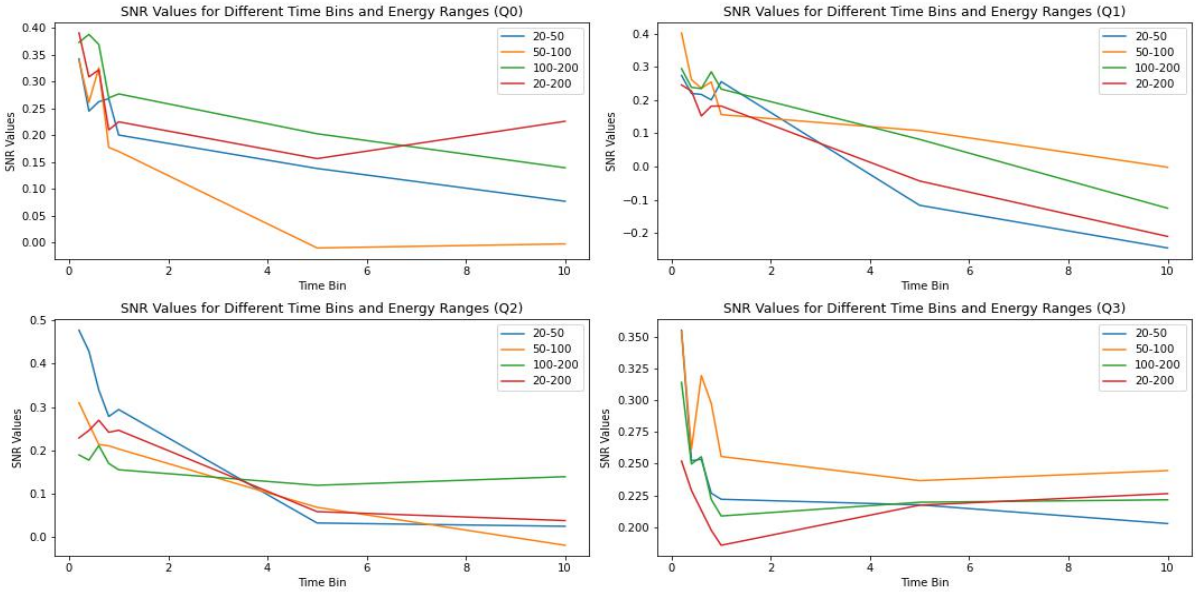


Figure 8.6: SNR vs time bin for non-grb window

The SNR graphs of both the suspected GRB region and non-GRB region show no distinct trend.

## 8.5 | Confidence Number

The ratio of the SNRnonGRB and SNRGRB value is around 0.62. Hence, a confidence value that can be associated to this detection of the GRB through this algorithm is 39.88%.

## 8.6 | Conclusion

The given detection is identified as a particle event by this algorithm and a confidence value of 39.88% can be associated to it even if it is considered to be a GRB event.